

Facilitating the Deployment of Next Billion IoT Devices with Distributed Antenna Systems

Xiaoran Fan

ox5bc@winlab.rutgers.edu
WINLAB, Rutgers University
North Brunswick, NJ, USA

ABSTRACT

Tiny IoT devices have shown their utilities in many fields. However, due to the low cost, small form factor, and inherently restricted computation resources, these IoT devices are facing many fundamental challenges such as the power issue, the communication issue, and the security issue when deployed in scale or operated in long-term period. In this paper, we discuss the feasibility of using distributed antenna systems to facilitate the deployment of IoT devices. Specifically, by coherently combining the phase of each antenna in a 3D distributed antenna system, we form an energy ball at the target location where the energy density level is significantly higher than the energy density level at any other locations. We highlight the properties of energy ball and deploy a testbed with over 20 software defined radios. Our preliminary results demonstrate that this energy ball has a great potential to be leveraged to solve many fundamental problems in IoT and enable exciting IoT applications.

CCS CONCEPTS

• **Hardware** → **Wireless devices**; • **Networks** → **Network reliability**.

KEYWORDS

Phased array; Wireless power transfer; Wireless security; Packet collision

ACM Reference Format:

Xiaoran Fan. 2019. Facilitating the Deployment of Next Billion IoT Devices with Distributed Antenna Systems. In *ACM MobiSys 2019 Rising Stars Forum (RisingStarsForum'19)*, June 21, 2019, Seoul, Republic of Korea. ACM, New York, NY, USA, 6 pages. <https://doi.org/10.1145/3325425.3329943>

1 INTRODUCTION

The Internet of Things (IoT) envisions an ubiquitous connectivity among billions of everyday objects. Today's IoT devices are energy efficient, consuming orders of magnitude lower power than the conventional sensors on computing, sensing, and communication. Today's IoT devices are also becoming increasingly smaller, which makes them deployable anywhere, on any item. *e.g.*, swallowed or injected into human body for vital signs monitoring [19], placed on

Permission to make digital or hard copies of all or part of this work for personal or classroom use is granted without fee provided that copies are not made or distributed for profit or commercial advantage and that copies bear this notice and the full citation on the first page. Copyrights for components of this work owned by others than ACM must be honored. Abstracting with credit is permitted. To copy otherwise, or republish, to post on servers or to redistribute to lists, requires prior specific permission and/or a fee. Request permissions from permissions@acm.org.

RisingStarsForum'19, June 21, 2019, Seoul, Republic of Korea

© 2019 Association for Computing Machinery.

ACM ISBN 978-1-4503-6776-9/19/06...\$15.00

<https://doi.org/10.1145/3325425.3329943>

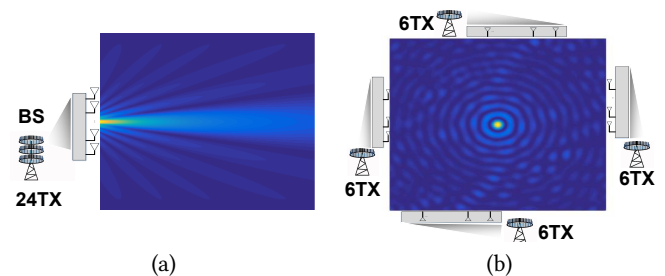


Figure 1: Comparison of the energy density heatmap generated by (a) a linear antenna array and (b) a distributed antenna array with the same number of antennas (24 in both cases). The receiver is placed at the center of the rectangular area.

a tiny insect for habitat monitoring [8]. While these IoT devices have proved their utilities in many ways, they are still facing fundamental challenges when deployed in scale or operated in long-term period. Specifically:

How to charge these tiny and battery-free IoT devices? Plugging them in or maintaining batteries are usually not feasible as these IoT devices may be deployed in an inaccessible environment (*e.g.*, volcano or swamp) or injected into the human body.

How to scale the ever-crowded wireless network to massive of these low-power IoT devices? While TDMA and FDMA are well understood, they require an accurate synchronization between the transmitter and the receiver and thus are not applicable in low-power IoT devices.

How to protect the communication confidentiality of these low-end IoT devices? The conventional jamming-based technique is not applicable since the power-constrained IoT sensors are unable to execute the computationally intensive interference cancellation operations.

These problems lie at the heart of the overall effort to scale up the IoT devices to satisfy an ever-growing user demand.

Recently, wireless access point designs are undergoing a major shift from co-located antennas to distributed antennas connected to a centralized processor for signal processing [2, 22]. The primary reason behind this shift is that the distributed antenna systems (DAS) achieve better spatial diversity, higher cell and network capacity, and scale better to the increasing number of end-devices [9, 25]. Today, major cellular providers like Verizon, AT&T, and Vodafone have already planned their DAS worldwide, *e.g.*, cloud radio access networks (C-RAN). In wireless local area networks (WLAN), we also witness the trend of Wi-Fi access points coupled with multiple extenders per geographical area. These spatially distributed transmitters/receivers essentially form a distributed antenna system.

Noticing the proliferation of distributed antenna systems in both global and local settings, in this paper we ask an important question – *is it possible to facilitate the deployment of IoT devices with distributed antenna systems?* Our discussion in this paper gives an affirmative answer and points out the way to achieve this: performing *beamforming* on distributed antenna systems, or *distributed beamforming* for short. Specifically, by coherently combining the phase of each antenna in a 3D distributed antenna system, we form an *energy ball* at the target location where the energy density level is significantly higher than the energy density level at any other locations¹. This energy ball differs from the conventional energy beam generated by the co-located antenna array, as shown in Figure 1. We describe one realization of this energy ball under unknown channel conditions and discuss its properties through both simulations and experiments. We envision at least three ways such energy ball can facilitate IoT deployment:

Efficient wireless charging. It is possible to power up in-body IoT devices using wireless signals. However, the main hurdle behind is that the excitation signals experience severe attenuation as they propagate in human tissues. Blindly amplifying the signal power is unfeasible due to the inherent health hazard. *e.g.*, skin burning. The state-of-the-art system, IVN [13], combines multiple signal streams transmitted over different frequencies to boost the received power at the target location under unknown channel conditions. However, this algorithm inevitably overheats the other parts of human bodies as well, which may inherently violate FCC’s regulation on RF exposure. In contrast, by leveraging the energy ball, we can increase the energy density level at the target location (*i.e.*, where the in-body IoT device stays) meanwhile avoiding overheating at other parts of the human body.

Scaling to concurrent transmissions. Another promising application of DAS is concurrent streams decoding. To understand how this works, let’s consider a simple case where multiple IoT devices transmit their sensing data to the gateway over the same channel. Assuming each antenna in the DAS can hear these concurrent streams and further pool them to the cloud. By coherently combining the phase on the cloud side, the DAS can intentionally receive the energy from the target transmitter while minimizing the received energy from the remaining transmitters. Hence it greatly improves the signal to interference-plus-noise ratio (SINR) of the target data stream, making it decodable at the cloud. Then by altering the phase combining plan on the cloud, the DAS could maximize the SINR of each data stream and decode them alternatively.

Secure IoT communication. By examining how the transmitter signals coherently combine at the receiver, we show that phase alignment accomplishes highly efficient secret communication against eavesdroppers without knowing their location, nor introducing any additional signal/noise. Also, to engage in secret communication, a distributed phase alignment system only needs to introduce very minor modifications to their normal transmission procedure. Once the transmitters’ phases are adjusted so that they are aligned at the receiver, they may start to communicate secretly to the receiver, by periodically dithering its phase around the proper alignment phase during transmission. In this way, the system naturally achieves secret communication. Firstly, the secret recipient’s SNR is largely

increased by aligning the phases at the intended recipient (and the SNR at eavesdroppers’ locations are significantly decreased). After the phase alignment is achieved, slight dithering of the phases has negligible impact on the alignment, but can create high received signal strength (RSS) variation at other locations, hindering anyone else from decoding the signal. Thirdly, it does not involve utilizing interference for secrecy, which complicates system design, requires complex interference cancellation and decoding schemes, which are unlikely to be allowed in practical systems.

In the following parts of the paper we first study the properties of the energy ball through both simulations and real-world experiments and we discuss the applicability of energy ball in different applications.

2 BEAMFORMING ON DAS

This section prepares the beamforming preliminary and discusses the properties of energy ball.

2.1 Beamforming Algorithm Sketch

Let us consider an N -antenna array that performs beamforming towards a target receiver. In free space, the received signal $R(t)$ and its power P can be represented as:

$$R(t) = e^{j\omega t} \sum_i^N \frac{a_i}{d_i} e^{j(\beta_i + \phi_i)}, \quad (1)$$

$$P = \left| \sum_i^N \frac{a_i}{d_i} e^{j(\beta_i + \phi_i)} \right|^2,$$

where a_i is the amplitude of the received signal sent from the i^{th} transmitter, and d_i is the distance between the receiver and the i^{th} transmitter antenna. Suppose there is no initial phase offset at each transmitter antenna. Let β_i be the phase value of the received signal sent from the i^{th} transmitter antenna. ϕ_i is the initial phase value of the signal sent from the i^{th} antenna, which is controllable at the transmitter side. The maximum signal power P is achieved when all the transmitted signals are *coherently combined* at the receiver side. Next we briefly review the beamforming algorithms under both known and unknown channel conditions.

Beamforming under known channel conditions. The most straightforward way to perform beamforming is to first measure the channel and then compensate the channel effect. Specifically, the receiver first sends a pilot tone to each transmitter antenna. Upon the detection of this pilot tone, each transmitter antenna computes the channel state information (CSI) and compensates the channel effect by multiplying each symbol to be sent with the transport conjugate of the CSI. The implicit assumption behind this method is the channel reciprocity, which requires all transmitter antennas to work in a dedicated Time Division Duplex (TDD) fashion². That is, both the transmitter and receiver should have an antenna that can switch between receiving and transmitting without re-locking its phase, which requires a specifically designed hardware that is not readily available on most low-cost IoT devices.

¹This energy ball maps to an energy disk in 2D space.

²Full duplex radio is desirable to align phases using the channel reciprocity, however it involves even more complex hardware and software design.

Beamforming under unknown channel conditions. One simple yet effective realization is the one-bit phase alignment algorithm proposed in [16, 17]. This algorithm runs in an iterative fashion, converging to the optimal phase combination without the need of channel measurement. Specifically, on each iteration, each transmitter antenna sets a random phase value. This random phase value is picked within $\pm\Phi^\circ$ of the phase value in previous iteration. All transmitters antennas are time synchronized and send out signals simultaneously. At the receiver side, multiple copies of the transmitter signals sent from different transmitter antennas combine together. The receiver measures the power of the combined signal and sends a one-bit feedback to transmitter antennas, indicating whether the current phase adjustment leads to a higher power or not. If yes, all transmitter antennas keep their phase settings; otherwise, they adopt the phase settings in previous iteration and perform a new round of phase adjustment. In either way, the antenna array retains the best phase combination it has attempted at the end of each iteration. This algorithm is proved to converge strictly to the optimal phase combination [17].

2.2 Understanding the Energy Ball

Two parameters are critical to the performance of distributed beamforming: the volume of energy ball and the energy efficiency. Motivated by the 3 dB beam width defined in conventional beamforming techniques [21], in this paper we use *3 dB energy ball width* to characterize the volume of energy ball. Formally, the 3 dB energy ball width is defined as the distance between the location with the highest energy and the location with the half of the highest energy. Furthermore, we use the *target to average energy ratio* to measure the energy efficiency of energy ball. The target to average energy ratio is formally defined as the ratio of the energy density at the target location to the average energy density at 10,000 locations that are uniformly sampled from a cube in 3D space, as shown in Figure 2. A higher target to average energy ratio indicates a more efficient energy focus. Next we conduct both simulations and real-world experiments to study the properties of energy ball. By default the transmitter sends the signal at 2.5 GHz band at a power of 1 watt. We use the free space model [6] to characterize the signal propagation in our simulations.

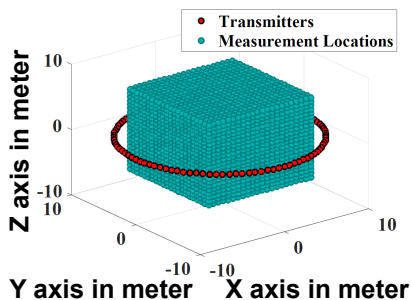


Figure 2: We measure the energy density level at 10,000 locations in a cubic space to determine the target to average energy ratio.

Impact of array size. We first study the impact of transmitter array size on the target to average energy ratio and 3 dB energy

ball width, respectively. In this simulation study, we arrange different number of transmitter antennas along a circle centered at the receiver on X-Y plane. The radius of this circle is 10 m. In each array size setting we compute the target to average energy ratio and the 3 dB energy ball width. The results are shown in Figure 3(a). We observe that the target to average energy ratio is quasi-linearly to the number of transmitter antennas. On the other hand, interestingly we observe that the 3 dB energy ball width quickly converges to 2.6 cm (in accordance with the theoretical optimal ball width $d_{3dB} \approx 0.22\lambda$) [21]) as we deploy more than nine transmitter antennas (shown in Figure 3(b)). The results clearly show that it is feasible to form a fine-grained energy ball using a reasonable amount of transmitter antennas.

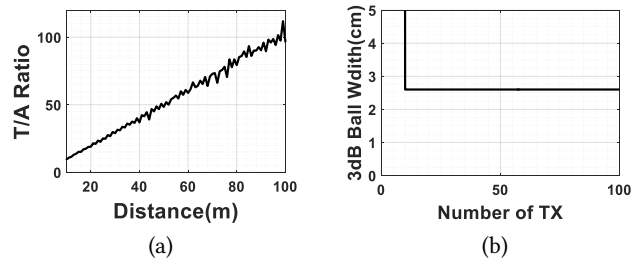


Figure 3: The impact of antenna array size on (a) the target to average energy ratio and (b) the 3 dB energy ball width. Transmitter antennas are deployed along the boundary of a circle centered at the receiver.

Further, we deploy an distributed antenna array with 24 antennas (consists of 16 USRP N210s and 4 USRP B210s) in an office building and measure the received power distribution in a $6\text{ m} \times 6\text{ m}$ rectangular area centered at the receiver. The transmission power is 71 mw (equivalent to 18.5 dBm). Figure 4(b) shows the power distribution over this rectangular area. We observe a clear energy peak at the receiver's location, indicating the received power at the receiver's location is considerably higher than the received power at any other locations in the field. This result clearly demonstrates the feasibility of forming an energy ball in real world settings.

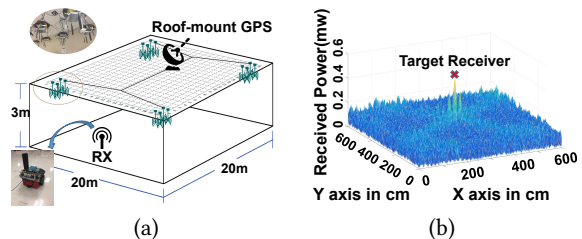


Figure 4: Examining the effectiveness of energy ball through real-world experiments. (a): the sketch of our 24 antenna based testbed. (b): the received power distribution in a $6\text{ m} \times 6\text{ m}$ rectangular area. The transmitter antennas are time synchronized through a GPS clock. A robot equipped with an omnidirectional dipole antenna (connected to a USRP N210) serving as the mobile receiver to sample the energy at each location.

Impact of receiver placement. We next investigate the impact of receiver placement on the target to average energy ratio and the 3 dB energy ball width through simulations. In these simulations, 100 transmitter antennas are evenly placed along the boarder of a circle centered at the receiver. The radius of this circle is 10 m. We move the receiver away from the center of this circle and observe the variation of the target to average energy ratio and the 3 dB energy ball width. The results are shown in Figure 5. As we can see from Figure 5(a), the target to average energy ratio increases dramatically as the receiver approaches to the boundary of the circle and then decreases as the receiver passes the circle boundary and moves away further. In terms of the ball size, we can see from Figure 5(b) that the 3 dB ball width stays the same as we move the receiver away from the center of this circle. Once the receiver passes the boundary of this circle and moves away further, the 3 dB ball width increases significantly.

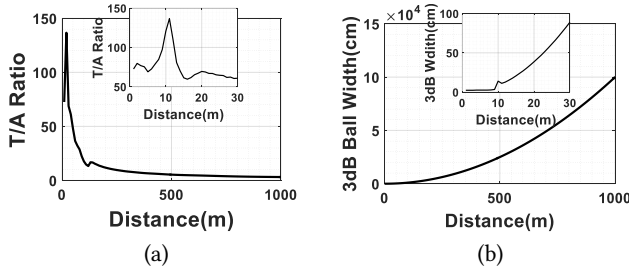


Figure 5: The impact of the distance between the transmitter area center and the receiver. We show (a) target to average energy ratios and (b) 3dB energy ball widths when we vary this distance from 0 to 1000m (and 0 to 30m). We have 100 transmitters that are placed along a 10 meter radius circle.

To understand this trend, we further plot the energy density distribution in four different receiver placement settings. As shown in Figure 6(a), we observe an energy peak at the receiver’s location when the receiver is placed in the center of the circle. The energy density levels at other locations are all very low due to the incoherent phase combining. As we move the antenna away from the center of the circle (but still within the boundary of this circle), we observe an energy peak at the receiver’s location as well despite a slight power decreasing, as shown in Figure 6(b). When the receiver moves out of the boundary of this circle, we can see the energy peak becomes insignificant, which in turn decreases the target to average energy ratio.

Impact of multipath. While the preceding explorations assume transmitter signals propagate in an ideal environment without any reflections, in this exploration we conduct a more realistic simulation by taking the multipath effect into consideration. Specifically, we employ Gaussian Wide Sense Stationary Uncorrelated Scattering model (GWSSUS) [15] to characterize the ambient environment. Each Line-of-sight (LoS) path and reflection path follow Rician fading model and Rayleigh fading model, respectively. The receiver signal is the combination of the signals propagates along both the LoS paths and reflection paths. We then change the number of multipath per transmitter-receive pair and explore its impact on the

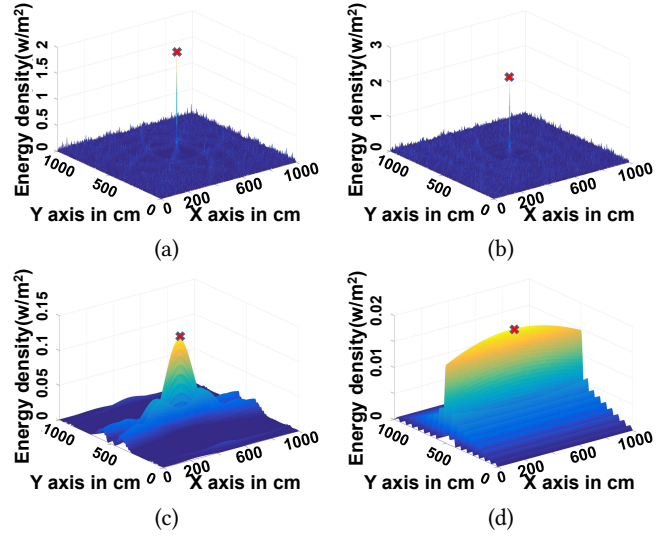


Figure 6: Detailed energy density distribution in a 10×10 meter area centered at the receiver for four specific transmitter-receiver placement settings: (a) receiver placed at the center of transmitter area; (b) receiver placed in the transmitter area, but not the center; (c) receiver placed outside of transmitter area, but close; (d) receiver placed further away to the transmitter area. The red x marks the energy density level at the target receiver.

target to average energy ratio and the 3 dB energy ball width. The results are shown in Figure 7. From Figure 7(a) we can see the target to average energy ratio first decreases as we increase the number of multipath per transmitter-receive pair to five, and then fluctuates as we increase the number of multi-path further. In terms of the 3 dB energy ball width, we can see it maintains a stable level as we gradually add more multi-paths on each transmitter-receiver pair. The results clearly demonstrate that the energy ball is not sensitive to multipath and hence could work in complex environment. This observation is also validated in our real-world experiments shown in figure 4.

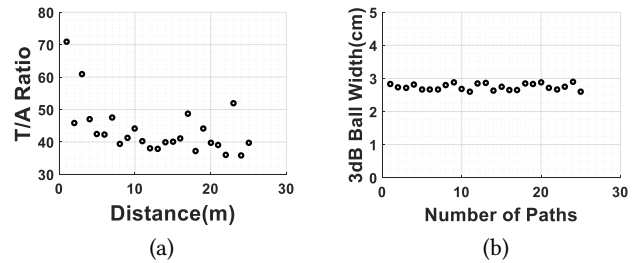


Figure 7: The impact of multipath effect on (a): the target to average energy ratio and (b): the 3 dB energy ball width. 100 transmitter antennas are evenly placed along the boundary of a circle centered at the receiver. The radius of this circle is 10 m.

3 AN EXPLORATION STUDY

We envision the energy ball could benefit IoT systems in multiple ways. Below we explore three important IoT applications: wireless charging, networking and communication confidentiality.

3.1 Wireless Charging for In-body IoT Devices

There is a growing trend on putting tiny IoT sensors/actuators into human bodies for vital sign monitoring, *e.g.*, monitoring heart and respiratory rates, or other medical purposes [19]. However, the miniature form factor of these IoT sensors prohibits the inclusion of batteries. Finding safe power transfer mechanisms to these sensors thus becomes a crucial research topic. Recent advance in wireless charging makes it possible to power up these in-body sensors remotely through wireless signals. The main hurdle, however, stems from the ultra-low charging efficiency: the excitation signals experience severe attenuation as they propagate through human tissues, blood and bones. For example, a 2.4 GHz RF signal attenuates over 50 dB after penetrating 6 cm human tissues [11]. Simply increasing the transmitting power does not solve the problem as it may likely lead to severe RF exposure and harm the human body.

An ideal wireless charging technology should be both safe and highly efficient. We envision energy ball could satisfy these rigid requirements. Specifically, as shown in Figure 1(b), the coherent phase combining leads to a high energy density level at a tiny spot surrounding the target location. The energy density level at other locations, however, is significantly lower, thus preventing overheating other areas of the body. Furthermore, the high target to average energy ratio indicates most of the energies concentrate on the target location, thus leading to a higher charging efficiency.

There are a few issues worth further investigation when applying energy ball for wireless charging:

Weak feedback. The correct execution of the energy ball algorithm relies on receiving the feedback from the IoT sensor. After penetrating human tissues, the in-body sensor’s feedback signal will attenuate to a power level that is below the noise floor, thus complicating the decoding. To address this challenge, we plan to leverage the LoRa backscatter [20] technology. Specifically, we replace the active radio in the IoT sensor with a passive radio and send a continuous sinusoidal tone as the excitation. The passive radio then encodes information by modulating the sinusoidal tone into a chirp signal and shifts this signal to another non-overlapping channel for collision avoidance. This modulation can be implemented with ultra low power RF components (*e.g.*, with an energy budget of several μw) and thus is suitable for in-body sensors. The received chirp signal, though below the noise floor, can be decoded due to the LoRa receiver’s ultra-high sensitivity, *i.e.*, -143 dBm [23].

Cold start. The other dilemma is that the in-body sensor needs to have sufficient energy to send out feedback signals before receiving any energy from our system. To solve this challenge, we can leverage the coherently-incoherent beamforming algorithm proposed by IVN [13], which guarantees that the sensor can be powered up within a given period of time. As soon as the delivered energy amount by the energy ball surpasses the energy requirement of the sensor, we can switch back to the normal feedback mechanism.

Unknown location. Usually these tiny IoT sensors are swallowed or injected into the human body, hence it is difficult to know

their exact location. The conventional RF localization schemes such as ArrayTrack [24], SpotFi [10], and RFind [14] do not work here because signals no longer travel along straight lines in this setting. Consequently, geometric principles needed by these localization algorithms do not hold. To localize these in-body sensors, we need to consider different refractions caused by human tissues, bones, and blood and build a more accurate in-body signal propagation model.

3.2 Enabling Concurrent Transmissions in Low-end IoT Networks

We envision the unique properties of the energy ball can also benefit the latest 802.11ax uplink MU-MIMO transmission without requiring synchronization among clients. Although uplink MU-MIMO has been specified in the latest 802.11ax standard [1], the tight time and frequency synchronization requirement – *i.e.*, the timing offset should be less than $0.4 \mu\text{s}$ and the carrier frequency offset should be less than 350 Hz – among clients remains a major barrier towards the wide adoption of uplink MU-MIMO. To achieve time synchronization, 802.11ax borrows the timing advance mechanism from cellular networks to adjust the transmission timing at each client. Also, it increases the cyclic prefix (CP) length of the OFDM symbols from $0.4 \mu\text{s}$ as in 802.11ac to $0.8 \mu\text{s}$. To achieve frequency synchronization, the clients need to adjust their internal frequency clocks by extracting the reference frequency from the trigger frames from the AP. These extra modules increase the protocol complexity as well as communication overhead. As a result, it has been very challenging to achieve tight time and frequency synchronization in a WAN environment.

Our early work [4] shows the feasibility of concurrent transmissions using the energy ball. Specifically, we expect the energy ball proposed in the future work can change the current uplink MIMO paradigm in the following aspects:

No uplink synchronization. In our distributed antenna setting, we completely bypass the time and frequency synchronization requirement. By exploring unique physical layer signatures (such as carrier frequency offset(CFO), CFO drifting) of low-end IoT clients, the APs search different combinations of phase adjustments of the signals received at distributed antennas to decode simultaneous transmissions from multiple clients. The intuition is that when the right phase combination is selected, only RF energy from one particular physical location can be clearly detected (thus only one client can be heard) while RF energies from other locations are minimized, mitigating the interference of transmissions from other clients. On the cloud, this process can be done concurrently for each IoT client.

Low overhead design. Furthermore, with smart phase adjustment done by cloud, we successfully enable uplink MU-MIMO as 802.11ax does and remove the channel sounding/feedback process and the need of reference sequences. This will greatly reduce the communication overhead and accordingly improve the throughput performance.

No blind spot decoding. The performance of traditional precoding methods degrades significantly when clients are physically close to each other (or when they are in the same direction with respect to the APs) because the channel similarity decreases the rank of the precoding matrix. Simply increasing the number of antennas

does not solve this problem. By distributing the same amount of antennas at different APs, the space resolution capability is greatly enhanced. The small size of the formed energy ball demonstrates that even the clients are very close to each other in 3D space, the MU-MIMO throughput performance is hardly affected.

3.3 Facilitating Communication Confidentiality in IoT Networks

Many IoT systems are deployed in critical settings that demand the communication to be decoded only by target receivers. Existing secret communication schemes leverage the broadcast nature of the wireless channel [7, 26] or directional beaming [12, 22] to introduce interference to hinder eavesdropping. These schemes either require the transmitters to know the eavesdroppers' locations or broadcast wideband noise that will interfere with the communication in the IoT networks.

We envision that the energy ball can serve as a viable solution to ensuring secret communications for IoT systems [5]. If we view the RF energy as information according to Shannon – Hartley theorem [18], then the ability to focus RF energy exactly at the intended receiver can help deliver secret bits exactly to the intended receiver. When applying the energy ball to achieve secret communication, we need to carefully address the following research challenges:

No Overhearing. The main challenge here is to ensure that no other IoT nodes can decode the secret message. In fact, we find that even nodes at other locations receive much weaker signals due to the energy ball, they are still able to decode the message. In order to make them completely “deaf”, we propose to increase the RSS variation at non-target locations. When the received signals have much lower RSS values and much higher RSS variations, the decodability of the message significantly drops if an amplitude-based modulation scheme such as PAM or QAM is used. In order to achieve higher RSS variations, we can periodically dither the transmitter phases around the proper alignment phase after achieving the initial phase alignment at the target receiver. We note that dithering the phases has the minimal effect on the target receiver's RSS values.

Moving Receiver. Another challenge occurs when the target receiver moves during the communication. In this case, a much faster phase alignment scheme is needed to adapt to the rapidly changing channel state. A promising solution is to let the receiver measure the channel in a timely manner and then leverage the property of channel reciprocity. This scheme however requires transmitters and receivers to work in a TDD fashion or all of them equipped with full duplex radios. In addition, the recent study in [3] shows that two close-band channels are correlated while their radio channels are changing. We can also leverage this property to achieve fast phase alignment in a simpler Frequency Division Duplex (FDD) fashion.

4 CONCLUSION AND FUTURE WORK

In this paper, we propose energy ball, a distributed beamforming scheme to facilitate the deployment of IoT devices. We study the important properties of energy ball through extensive simulations and experiments and discuss its applicability in three important applications, namely, wireless charging, wireless communication, and communication confidentiality. Our immediate next steps include prototyping and experimenting with larger arrays to solve the challenges and validate the outlined solutions in §3.

ACKNOWLEDGMENTS

I am grateful to the MobiSys'19 RisingStars Forum's reviewers for their constructive critiques, and Longfei Shangguan, Jie Xiong and Yanyong Zhang, for their invaluable comments, all of which have helped me greatly improve this paper.

REFERENCES

- [1] B. Bellalta. Ieee 802.11 ax: High-efficiency wlans. *arXiv preprint arXiv:1501.01496*, 2015.
- [2] L. Dai, S. Zhou, and Y. Yao. Capacity analysis in cdma distributed antenna systems. *IEEE TWC*, 2005.
- [3] X. Fan, H. Ding, S. Li, M. Sanzari, Y. Zhang, W. Trappe, Z. Han, and R. E. Howard. Energy-ball: Wireless power transfer for batteryless internet of things through distributed beamforming. *Proceedings of the ACM on Interactive, Mobile, Wearable and Ubiquitous Technologies*, 2(2):65, 2018.
- [4] X. Fan, Z. Qi, Z. Jia, and Y. Zhang. Enabling concurrent iot transmissions in distributed c-ran. In *Proceedings of the 16th ACM Conference on Embedded Networked Sensor Systems*, pages 390–391. ACM, 2018.
- [5] X. Fan, Z. Zhang, W. Trappe, Y. Zhang, R. Howard, and Z. Han. Secret-focus: A practical physical layer secret communication system by perturbing focused phases in distributed beamforming. In *IEEE INFOCOM 2018-IEEE Conference on Computer Communications*, pages 1781–1789. IEEE, 2018.
- [6] H. T. Friis. A note on a simple transmission formula. *Proceedings of the IRE*, 34(5):254–256, 1946.
- [7] S. Gollakota and D. Katabi. Physical layer wireless security made fast and channel independent. 2011.
- [8] J. James, V. Iyer, Y. Chukewad, S. Gollakota, and S. B. Fuller. Liftoff of a 190 mg laser-powered aerial vehicle: The lightest wireless robot to fly. In *ICRA*, 2018.
- [9] R. K. Sheshadri, M. Y. Arslan, K. Sundaresan, S. Rangarajan, and D. Koutsonikolas. Amorf: amorphous wifi networks for high-density deployments. In *CoNEXT*, 2016.
- [10] M. Kotaru, K. Joshi, D. Bharadia, and S. Katti. Spotfi: Decimeter level localization using wifi. In *SIGCOMM*, 2015.
- [11] D. Kurup, W. Joseph, G. Vermeeren, and L. Martens. In-body path loss model for homogeneous human tissues. *IEEE Transactions on Electromagnetic Compatibility*, 2012.
- [12] L. Liu, R. Zhang, and K.-C. Chua. Secrecy wireless information and power transfer with miso beamforming. In *Global Communications Conference (GLOBECOM), 2013 IEEE*, pages 1831–1836. IEEE, 2013.
- [13] Y. Ma, Z. Luo, C. Steiger, G. Traverso, and F. Adib. Enabling deep-tissue networking for miniature medical devices. In *SIGCOMM*, 2018.
- [14] Y. Ma, N. Selby, and F. Adib. Minding the billions: Ultra-wideband localization for deployed rfid tags. In *MOBICOM*, 2017.
- [15] U. Martin and M. Grigat. A statistical simulation model for the directional mobile radio channel and its configuration. In *Spread Spectrum Techniques and Applications Proceedings, 1996., IEEE 4th International Symposium on*, volume 1, pages 86–90. IEEE, 1996.
- [16] R. Mudumbai, J. Hespanha, U. Madhow, and G. Barriac. Scalable feedback control for distributed beamforming in sensor networks. In *Proceedings of IEEE ISIT*, 2005.
- [17] R. Mudumbai, B. Wild, U. Madhow, and K. Ramchandran. Distributed beamforming using 1 bit feedback: from concept to realization. In *Proceedings of Citeseer Allerton, 2006*.
- [18] C. E. Shannon, W. Weaver, and A. W. Burks. The mathematical theory of communication. 1951.
- [19] A. Swiston Jr, G. A. Ciccarelli, G. Traverso, S. Schwartz, T. Hughes, T. Boettcher, R. Barman, and R. Langer. Physiologic status monitoring via the gastrointestinal tract. Technical report, 2015.
- [20] V. Talla, M. Hesar, B. Kelloog, A. Najafi, J. R. Smith, and S. Gollakota. Lora backscatter: Enabling the vision of ubiquitous connectivity. *Proceedings of the ACM on Interactive, Mobile, Wearable and Ubiquitous Technologies*, 2017.
- [21] T. E. Tuncer and B. Friedlander. *Classical and modern direction-of-arrival estimation*. Academic Press, 2009.
- [22] J. Wang, H. Zhu, and N. J. Gomes. Distributed antenna systems for mobile communications in high speed trains. *IEEE JSAC*, 2012.
- [23] LoRa specification. Website.
- [24] J. Xiong and K. Jamieson. Arraytrack: a fine-grained indoor location system. In *NSDI*, 2013.
- [25] J. Xiong, K. Sundaresan, K. Jamieson, M. A. Khojastepour, and S. Rangarajan. Midas: Empowering 802.11 ac networks with multiple-input distributed antenna systems. In *CoNEXT*, 2014.
- [26] A. Yener and S. Ulukus. Wireless physical-layer security: Lessons learned from information theory. *Proceedings of the IEEE*, 103(10):1814–1825, 2015.